



PRR repeats in the intracellular domain of KISS1R are important for its export to cell membrane.

Lucie Chevrier, Alexandre de Brevern, Eva Hernandez, Jérôme Leprince,
Hubert Vaudry, Anne Marie Guedj, Nicolas de Roux

► To cite this version:

Lucie Chevrier, Alexandre de Brevern, Eva Hernandez, Jérôme Leprince, Hubert Vaudry, et al.. PRR repeats in the intracellular domain of KISS1R are important for its export to cell membrane.: PRR repeats in intracellular domain of KISSIR. Mol Endocrinol, 2013, 27 (6), pp.1004-14. 10.1210/me.2012-1386 . inserm-00926577

HAL Id: inserm-00926577

<https://www.hal.inserm.fr/inserm-00926577>

Submitted on 23 Apr 2014

HAL is a multi-disciplinary open access archive for the deposit and dissemination of scientific research documents, whether they are published or not. The documents may come from teaching and research institutions in France or abroad, or from public or private research centers.

L'archive ouverte pluridisciplinaire **HAL**, est destinée au dépôt et à la diffusion de documents scientifiques de niveau recherche, publiés ou non, émanant des établissements d'enseignement et de recherche français ou étrangers, des laboratoires publics ou privés.

PRR repeats in the intracellular domain of KISS1R are important for its export to cell membrane

Running title: PRR repeats in intracellular domain of KISS1R

Lucie Chevrier¹, Alexandre de Brevern², Eva Hernandez¹, Jérôme Leprince³, Hubert Vaudry³, Anne Marie Guedj⁴, Nicolas de Roux^{1,5}.

¹ INSERM UMR676, Univ Paris Diderot, Sorbonne Paris Cité, F-75739 Paris, France

² INSERM UMR-S 665; Univ Paris Diderot; Sorbonne Paris Cité; INTS; Laboratoire d'Excellence GR-Ex, 75015 Paris, France.

³ INSERM UMR982, Univ Rouen, Mont-Saint-Aignan, France

⁴ Service des Maladies Métaboliques et Endocriniennes, Hôpital Carémeau, Nîmes

⁵ Laboratoire de Biochimie. Hôpital Robert Debré. 75019 Paris.

Corresponding author: Nicolas de Roux, INSERM U676, Hôpital Robert Debré, 48 Bd Sérurier, 75019 Paris, France, tel.: + 33 (0)1 40 03 19 85; Fax: + 33 (0)1 40 03 19 95; E-mail: nicolas.deroux@inserm.fr.

To whom correspondence should be addressed: Nicolas de Roux, INSERM U676, Hôpital Robert Debré, 48 Bd Sérurier, 75019 Paris, France, tel.: + 33 (0)1 40 03 19 85; Fax: + 33 (0)1 40 03 19 95; E-mail: nicolas.deroux@inserm.fr.

Keywords: KISS1R, IHH, PolyProline II helix

Disclosure statement: The authors have nothing to disclose.

ABSTRACT

Inactivating mutations of KISS1R have been recently described as a rare cause of isolated hypogonadotropic hypogonadism (IHH) transmitted as a recessive trait. Few mutations have been described and the structure-function relationship of KISS1R remains poorly understood. Here, we have taken advantage of the discovery of a novel mutation of KISS1R to characterize the structure and function of an uncommon protein motif composed of three proline-arginine-arginine (PRR) repeats located within the intracellular domain. A heterozygous insertion of one PRR repeat in-frame with three PRR repeats leading to synthesis of a receptor bearing 4 PRR repeats (PRR-KISS1R) was found in the index case. Functional analysis of PRR-KISS1R showed a decrease of the maximal response to kisspeptin stimulation, associated to a lower cell surface expression without modification of total expression. PRR-KISS1R exerts a dominant negative effect on the synthesis of the wild type KISS1R (WT-KISS1R). This effect was due to the nature of inserted residues, but also to the difference of the length of the intracellular domain between PRR- and WT-KISS1R. A molecular dynamic analysis showed that the additional PRR constrained this arginine rich region into a polyProline type II helix. Altogether, this study shows that a heterozygous insertion in KISS1R may lead to IHH by a dominant negative effect on the WT receptor. An additional PRR repeat into a proline-arginine rich motif can dramatically changed the conformation of the intracellular domain of KISS1R and its probable interaction with partner proteins.

INTRODUCTION

Isolated hypogonadotropic hypogonadism (IHH) is defined by low sex steroid hormone synthesis with low LH and FSH levels. The congenital form of this condition is a rare disease. Several genes have now been linked to IHH. Some were natural candidate genes, such as those encoding for the GnRH receptor (1) or its ligand, GnRH (2). Others were characterized by genome mapping and encoded for Kisspeptins (Kp) (3) and their receptor (KISS1R) (4, 5) or Neurokinin B (NKB) and its receptor (TACR3) (6). Kp and NKB are both neuropeptides expressed in hypothalamic neurons as well as their receptors. They belong to a complex neuroendocrine network aiming to control synthesis and secretion of GnRH. They are major determinants of the gonadotropic axis reactivation leading to pubertal onset (7). They also relay the estradiol positive- and negative-feedback on the gonadotropic axis leading to the LH ovulatory peak (8, 9).

KISS1R is a G-protein coupled receptor (GPCR) expressed in GnRH neurons (9). Kp activates phospholipase C beta and MAPK signaling pathways and depolarize GnRH neurons by activating nonselective TRPC cation channels and by inhibiting inwardly rectifying potassium channels (9).

To date, 11 mutations in *KISS1R* have been identified in IHH (4, 5, 10-15). IHH due to KISS1R mutations is transmitted as a recessive trait although late puberty has been reported in heterozygous parents of at least one index case (4). Compound heterozygous mutations (5, 12) or homozygous mutations have been reported (4, 5, 10, 11, 14, 15). However, there are no striking genotype-phenotype correlations for KISS1R mutations. Complete loss-of-function mutations do not necessarily cause complete gonadotropic deficiency and variable phenotypes could be observed in patients carrying the same KISS1R mutation (4, 14). Similar reproductive phenotype variability was also reported in *Kiss1*-deleted mouse model (16, 17). In very few cases, one heterozygous mutation in *KISS1R* was shown to be associated with a mutation in other IHH genes (18).

In the present study, we identified a heterozygous variant in *KISS1R* in one patient harboring IHH. This variant is characterized by the addition of one proline and two arginines (PRR) in the intracellular domain of the receptor. The absence of a second event on the other allele, the normal coding sequence in other IHH genes, and the uncommon location of the insertion in the intracellular domain of KISS1R led us to suspect that the mutated receptor may have a dominant negative effect on

the WT KISS1R. Moreover, this PRR repeat motif seemed unique in mammals and its biochemical function, if any, was unknown. We have therefore analyzed the functional effects of the PRR insertion in the intracellular domain of KISS1R and modeled the structural consequence of this insertion. Functional results were then correlated with the phenotype.

MATERIALS AND METHODS

Patient. The proband was a 16-year-old boy who was referred for impuberism and obesity. He was born at term and there was no history of cryptorchidism. At the initial presentation, he was Tanner stage 1. The BMI was 31 kg/m². His penis length was 5 cm, and right and left testicular volumes were 3 ml. There was no anosmia. The birth age was 13 yrs. He reported episodic nocturnal enuresis. Laboratory investigations revealed low plasma testosterone levels (1 nmol/L) with low LH (2.9 IU/L) and low FSH (5.3 IU/L) levels. The other endocrine axes were normal. The family history revealed obesity in the mother and the sister and a fertility problem in the father, but it was not possible to obtain further details.

Mutation analyses. The sequencing of *KISS1R* exons have been performed from DNA extracted from blood lymphocytes as previously described (4). Briefly, the five exons of *KISS1R* were amplified by PCR, and the PCR products were sequenced with BigDye dideoxyterminator cycle sequencing kit and the 3100 sequencer (Applied Biosystems) with the same primers. Both parents gave informed consent for genetic analysis of the proband's DNA but after the characterization of the mutation in the proband, they did not agree to determine whether the mutation was de-novo or was transmitted by one of them or to the proband's sister.

Cell culture. HEK-293, Cos-7 and HeLa cells were cultured in high glucose (4,500 mg/liter) DMEM with GlutaMAX™ I (Invitrogen, Cergy Pontoise, France), supplemented with 10% FCS, 100 U/ml penicillin and 100 µg/ml streptomycin (Invitrogen), and 25 mM Hepes. Cells were incubated in a humidified 95% air, 5% CO₂ controlled atmosphere at 37°C. Medium was changed every 3 or 4 days. Passages were performed once per week, using 1X trypsin/EDTA (Invitrogen).

Construction of the expression vectors. The PRR insertion was introduced by PCR into the wild type *KISS1R* sequence cloned in a pcDNA3.1 expression vector (WT-KISS1R) (Table 1) as described elsewhere (14). Briefly, the mutation was reproduced by PCR, then the PCR fragment was cut by the restriction enzymes SbfI and PpuMI (New England Biolabs, Evry, France) and was subcloned into a KISS1R-expressing vector in place of the WT sequence. The resulting vector was called PRR-KISS1R. To study cell surface expression of KISS1R, a HA epitope (YPYDVPDYA) was added at the N-terminal end of KISS1R after the initial methionine (11). The resulting plasmid was called WT-HA-KISS1R. The vector expressing a HA-tagged PRR mutated KISS1R (PRR-HA-KISS1R) was constructed by exchanging a HindIII-BsrGI fragment from PRR-KISS1R into WT-HA-KISS1R.

For the construction of (AAA)₄-, AAA(PRR)₃- and (PRR)₃AAA-KISS1R expressing vectors, in which the 4 PRR repeats were replaced respectively by AAAAAAAAAA, AAAPRRPRRPRR and PRRPRRPRRAAA, a fragment with SbfI, BamHI and KpnI, HindIII restriction sites were synthesized, and inserted in pUC57 cloning vector between KpnI and HindIII restriction sites (Eurogentec, Angers, France). Next, fragments of interest were cut by the restriction enzymes SbfI and BamHI (New England Biolabs) and were subcloned into KISS1R- or HA-KISS1R-expressing vectors in place of the WT sequence.

To construct the vector expressing a KISS1R without the PRR repeats, ΔPRR-HA-KISS1R or ΔPRR-KISS1R, a SbfI-BamHI fragment containing a SfaAI restriction site was amplified by PCR from the WT receptor and subcloned into HA-KISS1R- or KISS1R-expressing vector at SbfI and BamHI sites. This plasmid was cut by SfaAI, incubated with T4 DNA polymerase (New England Biolabs) to remove the 3' cohesive extremity and generate blunted extremities, and then incubated with T4 DNA ligase (New England Biolabs) to obtain ΔPRR-HA-KISS1R and ΔPRR-KISS1R plasmids.

Plasmid constructs were validated by direct sequencing of the inserted fragments and by restriction-enzyme mapping.

Transfection. HEK-293, Cos-7 and HeLa cells were seeded in 35-mm dish. Twenty-four hours after plating, cells were transfected with expression vectors using FuGENE HD (Roche Diagnostics,

Meylan, France) or using the calcium phosphate transfection kit (Invitrogen) according to the manufacturer's instructions.

Inositol phosphate (IP) measurements. Twenty-four hours post-transfection, cells were seeded in 96-well plates at a density of 20,000 cells/well. After 24 h (48 h post-transfection), total IP was measured using the IP-One HTRF® Assay kit (Cisbio Bioassays, Bagnols-sur-Cèze, France) according to the manufacturer's instructions. Briefly, cells were stimulated with Kp10 during 1 h at 37°C. After stimulation, the fluorophore d2-labeled IP1 and anti-IP1 antibody conjugated to cryptate (IP-one Tb) were added for 1 h at room temperature, and the plate was read at 620 nm and 665 nm using PARADIGM™ Detection Platform (Beckman Coulter, Brea, CA). Each functional analysis was performed in triplicates.

MAPK activation. Twenty-four hours after transfection, HeLa cells were serum-starved for 18 h. Cells were treated with Kp10 at 10^{-5} M in DMEM supplemented with 0.2% BSA during 10 min. Total proteins were extracted with "Cell Lysis Buffer" (Cell Signaling, Danvers, MA) according to the manufacturer's instructions. Thirty µg of proteins were resolved in 10% SDS-PAGE and electroblotted for 1 h at 100 V, onto Hybon-P membranes (GE Healthcare, Velizy, France). Membranes were blocked 3 h at room temperature, by using 5% non-fat milk in TBS containing 0.1% Tween 20 (TBST) and incubated overnight at 4°C with a mouse monoclonal anti-phospho-p44/42MAPK antibody (Cell Signaling) diluted in blocking solution. Membranes were washed 3 x 10 min at room temperature in TBST, incubated for 1 h with a peroxidase-conjugated Fab specific Goat anti-Mouse IgG (Sigma-Aldrich, Saint-Quentin Fallavier, France) in blocking solution, and washed again with TBST. Bound antibodies were revealed by chemiluminescence with the Immun-Star™ WesternC™ Chemiluminescent Kit (Biorad, Marne-la-Coquette, France) using ChemiDoc™ XRS (Biorad). After stripping of bound antibodies, membranes were probed again with a monoclonal mouse anti-p44/42MAPK antibody (Cell Signaling) according to the same procedure.

KISS1R quantification by ELISA. Twenty-four hours post-transfection, cells were seeded in 96-well plates at a density of 30,000 cells/well. Twenty-four hours later, cells were washed with PBS, fixed with 2% paraformaldehyde (PFA) for 10 min at room temperature. To quantify the total cellular expression of KISS1R, cells were permeabilized with 0.2% Triton X-100 (Sigma-Aldrich) for 10 min, washed and then blocked with PBS supplemented with 2% BSA (Sigma-Aldrich). Cells were incubated with the monoclonal rat anti-HA antibody 3F10 (Roche Diagnostics) at 0.5 µg/ml in PBS supplemented with 1% BSA for 1 h at room temperature. After three washes with PBS, cells were incubated with a goat anti-rat antibody coupled to horseradish peroxidase (Jackson Immuno-Research, Suffolk, England) at 0.2 µg/ml in PBS-1% BSA. Signal was detected and quantified with “BM Chemiluminescence ELISA Substrate POD” (Roche Diagnostics) using Paradigm counter (Beckman coulter). For cell surface quantification, the protocol was the same, with the exception that cells were not permeabilized. Each analysis was performed in triplicates.

Molecular dynamics of WT-KISS1R and PRR-KISS1R fragment. Protein structure fragments encompassing PRR repetitions of WT-KISS1R and PRR-KISS1R have been analyzed through molecular dynamics approach. A detailed description of the method may be found in the supplementary data. Fragments were of 24-residue length for the WT sequence and 27-residue length for the PRR sequence and were respectively named (PRR)₃ and (PRR)₄. Five structural models for (PRR)₃ and five for (PRR)₄ were built using I-Tasser webserver (19). In addition, each model was constrained to add PolyProline II (PPII) helix conformation (20), leading to 20 independent structural models (10 for (PRR)₃ and 10 for (PRR)₄). Molecular dynamics simulations were performed with GROMACS 4.0.5 software (21) for each protein fragment. The structural models were also analyzed using secondary structure assigned with DSSP software (22) and a refined approach named Protein Blocks (PBs) analysis (23). This latter approach allowed a precise comparative analysis of conformations of (PRR)₃ and (PRR)₄ (24). It was also used to compute the entropy termed N_{eq} , which quantifies the stability of local protein conformations.

Statistical analysis. Data were analyzed using GraphPad Prism Software (GraphPad, San Diego, CA)

by one-way ANOVA with a Bonferroni test if number of groups was superior to 2 (Figure 2B, 4, 6B, 7) or by a two tails Student's t-test when 2 groups were compared (Figure 3). Differences were considered significant when $p < 0.05$. For IPs measurements and MAPK activation, results are expressed as percentage of maximal stimulation of WT-KISS1R, which was set at 100%. In all figures reporting KISS1R quantification, the expression of mutated receptors was expressed as percentage of WT-KISS1R expression.

RESULTS

Sequencing analysis. Sequencing of the coding exons of *KISS1R* revealed a heterozygous in-frame insertion of 9 nucleotides at position 1023 (c.1023Ins9) (Figure 1A). The c.1023Ins9 allele encoded for a KISS1R with an additional PRR repeat in a proline-arginine-rich region of the intracellular domain at residue 342. It led to the synthesis of a receptor with 4 consecutive PRR repeats instead of 3 (Figure 1B). This mutant receptor was called “PRR-KISS1R”. The DNA of the parents and the sister of the proband were not available for analysis.

Functional analyses. To study the effect of the PRR insertion on KISS1R function, a PRR-KISS1R encoding plasmid was transiently transfected in HeLa cells and Kp10-induced generation of intracellular IP was quantified. Forty-eight hours after transfection, no Kp10-induced increase in IP was observed in control cells transfected with the empty vector. In cells transiently expressing WT-HA-KISS1R, Kp10 increased intracellular IPs (Figure 2A). In PRR-HA-KISS1R-expressing cells, Kp10 also induced an intracellular increase of IPs (Figure 2A). However, the maximal effect of Kp10 stimulation was lowered by $46 \pm 1\%$ in PRR-HA-KISS1R-expressing cells as compared to WT-HA-KISS1R-expressing cells. Moreover, the EC50 in PRR-HA-KISS1R-expressing cells was slightly increased by 1.8 fold ($9.8 \pm 1.0 \times 10^{-7}$ M for PRR-HA-KISS1R vs $5.3 \pm 1.3 \times 10^{-7}$ M for WT-HA-KISS1R). To ensure that the HA-tag did not modify the activity of the receptors, Kp10-induced generation of IP in tagged and untagged WT-KISS1R and PRR-KISS1R transiently transfected cells were compared. Similar Kp10-induced IP increase was observed, indicating that the HA-tag did not alter KISS1R activation (data not shown).

Kp was known to activate the MAPK pathway (25). To study KP10-induced activation of the MAPK pathway, WT-HA-KISS1R and PRR-HA-KISS1R transiently transfected HeLa cells were incubated with 10^{-5} M of Kp10 for 10 min. Total proteins were extracted, immunoblotted with anti-phospho-MAPK antibody (P-MAPK) and then with anti-MAPK antibody. Kp-induced MAPK phosphorylation was significantly lower in PRR-HA-KISS1R-expressing cells than in WT-HA-KISS1R-expressing cells (Figure 2B). To verify that the difference observed between WT and PRR-KISS1R was not cell-type specific, we reproduced these functional analyses in HEK293 and Cos-7 cell lines. Data confirmed that the maximal Kp10-stimulation of intracellular IP accumulation and of the MAPK pathway was significantly lower in PRR-HA-KISS1R-expressing cells than in WT-HA-KISS1R-expressing cells (data not shown).

Cell surface quantification by ELISA. Functional analyses showed that the PRR insertion impaired the activation of the receptor and the maximal stimulation of KISS1R by Kp10. The difference between WT-KISS1R and PRR-KISS1R could thus be due to a lower amount of PRR-KISS1R expressed at the cell surface. To analyze cell surface expression of PRR-HA-KISS1R, the HA-tag was quantified by ELISA in non-permeabilized (cell surface expression) and in permeabilized (total expression) transiently transfected HeLa cells. Cell surface expression of PRR-HA-KISS1R was significantly decreased by 2-fold compared to WT-HA-KISS1R (Figure 3A). Total expression did not significantly change between PRR-HA-KISS1R and WT-HA-KISS1R (Figure 3B). These results indicate that the additional PRR impaired the intracellular trafficking of KISS1R. We also tested the effect of the PRR insertion on the internalization of KISS1R. In HEK293 cells, the PRR insertion did not modify the constitutive internalization of KISS1R as well as Kp10-induced internalization (data not shown).

Effect of PRR-KISS1R on WT-HA-KISS1R expression. As the PRR insertion was found heterozygous in the affected patient, and isolated gonadotropic deficiency due to KISS1R mutation is usually transmitted as a recessive trait, we suspected that the PRR-KISS1R could decrease the expression of the WT receptor at the cell surface and therefore act as a dominant negative receptor on WT-KISS1R. For that purpose, WT-HA-KISS1R was co-expressed in HeLa cells with untagged PRR-KISS1R by

transient transfection. The expression of WT-HA-KISS1R was subsequently quantified by ELISA. The co-expression of WT-HA-KISS1R with PRR-KISS1R in HeLa cells resulted in a reduced amount of WT-HA-KISS1R at the cell surface (Figure 4A). This reduction was significantly different with two fold more of untagged PRR-KISS1R than WT-HA-KISS1R alone. Cell surface expression of PRR-HA-KISS1R co-expressed with increasing amounts of untagged PRR receptor was also quantified. Co-expression of PRR-HA-KISS1R with PRR-KISS1R only slightly reduced its cell surface expression (Figure 4A). The total expression of WT-HA-KISS1R co-transfected with two fold more PRR-KISS1R was significantly reduced by 2-fold (Figure 4B), whereas the total expression of PRR-HA-KISS1R was only slightly perturbed by the increasing amount of co-transfected PRR-KISS1R. The ratio of the cell surface expression to the total expression of the WT-KISS1R was therefore not modified by the co-transfection with PRR-KISS1R (Figure 4C). In addition to have an altered intracellular trafficking, PRR-KISS1R also disturbed the total expression of WT-KISS1R.

Molecular dynamics. To understand the impact of the additional PRR in the conformation of the intracellular domain, we analyzed the protein dynamics using classical approaches (26). No structure was available in the Protein Databank (27) and no related proteins with available structure can be found. We have thus focused the analysis on protein fragments encompassing the PRR repeats, *i.e.*, a fragment of 24 residues for WT-KISS1R ((PRR)₃) and 27 residues for PRR-KISS1R ((PRR)₄) (Figure S1A). No available structure or homologue was found for this sequence. Secondary structure prediction methods (*e.g.*, PSI-PRED (28)) predicted coil with a poor accuracy but also a flexible region (data not shown) (29).

I-Tasser webserver (30) was used to propose structural models for both fragments. According to the I-Tasser's C-scores, the best 5 structural models for (PRR)₃ and for (PRR)₄ have been conserved. As the proline rich region was often seen as a PPII helix (31), we also tested models with PRR repeats constrained as PPII helices using the Modeller software (32). The structural models with the lowest DOPE score were selected. Hence, each protein fragment was represented by 5 *free* structural models, *i.e.*, without PPII helices, and 5 constrained structural models, *i.e.*, with PPII helices. A first analysis

in terms of secondary content showed that 95% of the structure corresponded to a coil state according to DSSP assignment.

A molecular dynamic analysis was performed for the 20 different structural models for at least 50 ns. As expected, the two protein fragments were highly dynamic. The first visual analysis showed a compaction of the WT fragment. To quantify this compaction, distances between the extremities of (PRR)₃ or (PRR)₄ were computed. At first, all structural models of (PRR)₃ (*free* and PPII *constrained*) showed both a rapid and irreversible decrease in the distance between extremities (Figure 5A). On average, the distance was 5 Å. In contrast, (PRR)₄ structural models (*free* and PPII *constrained*) showed a higher distance between extremities that remained around 20 Å.

To analyze the conformations of the peptide more in-depth, a structural alphabet was used (33), *i.e.*, a set of small local protein structures that can be used to approximate every part of a protein structure. The structural alphabet used for this analysis, namely Protein Blocks (PBs) (23, 24), is composed of 16 distinct prototypes that are 5 residues in length. The analysis of (PRR)₃ by the structural alphabet revealed four consecutive regions (R1 to R4) (Figure 5B, left panel). R1 was highly fuzzy, mainly associated to helical PBs (PBs *m* is the core of helix). R2 was associated to PBs related to beta-strands (PBs *b* to *d*). R3 was less fuzzy, but not associated to beta conformations, only two residues preferred PBs *c* while most of the others were more associated to turns (succession of PBs *fl* and *d*). R4 was fuzzier than R3 with tendencies to beta-strands PBs. The analysis of (PRR)₄ by the structural alphabet showed a strong preference for the PBs *d* (Figure 5B, right panel). Both R1 and R2 were in beta conformation, but not beta-sheets. The adjunction of one PRR repeat showed a striking constraint of R3 with only PBs *d* for the last PRR repeat. It was the core of the PPII helix. R4 showed an accented transition (PBs *fbe/gc*).

To quantify constraints, the PB distribution was transformed in a quantitative value (N_{eq}). If only one PB was observed for a residue, N_{eq} equals to 1; if all PBs were predicted with the same probability, N_{eq} equals to 16. At the N-terminus of the analyzed sequences (R1 and R2), N_{eq} were lower for (PRR)₄ fragment than for (PRR)₃ (Figure 5C). Then, N_{eq} were roughly comparable for the two first PRR repeats. The addition of one repeat induced a high constraint with a N_{eq} close to 1. The C-terminus of both sequences had higher N_{eq} , but again N_{eq} was lower for (PRR)₄ than for (PRR)₃.

From these results, it should be noted that (PRR)₃ was highly flexible and did not possess a PPII helix, having only few positions that were stable, which were comparable to turns. The adjunction of an extra PRR repeat created a strong rigidity of the peptide, with conformation into a PPII helix. The content of PPII helix of structural models of (PRR)₃ (*free* and *PPII constrained*) was very limited (less than 3%), while the PPII helix content of (PRR)₄ structural models (*free* and *PPII constrained*) was always high and especially for the last PRR repetition (more than 85%).

Implication of the proline and arginine-rich domain in KISS1R expression. To study how the PRR insertion interferes with the normal function of KISS1R, mutants of the PRR repeat were constructed (Table 1). We tested the nature of the inserted residues as well as the position of the insertion of the triplet in regards to the normal PRR repeat. Substitution of the PRR insertion by AAA at the N-terminal of the PRR repeat (AAA(PRR)₃) slightly increased the EC50 by 1.2 fold ($1.5 \pm 1.1 \times 10^{-7}$ M for WT-HA vs $1.9 \pm 1.0 \times 10^{-7}$ M for AAA(PRR)₃) and decreased maximal stimulation by 30% (Figure 6A). This maximal decrease of IP generation was associated with a decrease of the total and cell surface expression (Figure 6B). Interestingly, addition of an AAA at the C-terminal end of the PRR repeat ((PRR)₃AAA) did not change the EC50 value nor the maximal stimulation of the mutant receptor (Figure 6A). A slight decrease of cell surface and total expression was observed for (PRR)₃AAA-KISS1R when compared to WT-KISS1R (Figure 6B). To definitively affirm the functional importance of the PRR repeats, the 4 PRR repeats were substituted by alanines ((AAA)₄) or deleted (Δ PRR; only the last arginine was conserved). The absence of PRR repeats by deletion or AAA substitution induced an increase of the EC50 ($1.5 \pm 1.1 \times 10^{-7}$ M for WT-HA vs $8.2 \pm 0.8 \times 10^{-7}$ M for (AAA)₄ and $1.1 \pm 0.8 \times 10^{-6}$ M for Δ PRR) and a decrease of the maximal stimulation. Overall, ratios of cell surface expression/total expression of these mutated receptors were not changed (Figure 6B). The dominant negative effect of each mutant on WT-KISS1R expression was then tested by co-expression in HeLa cells. (AAA)₄, AAA(PRR)₃ and Δ PRR-KISS1R decreased the total expression of WT-HA-KISS1R ($64 \pm 16\%$, $72 \pm 16\%$ and $69 \pm 10\%$ of the total expression in absence of the mutated receptors respectively) (Figure 7). Cell surface expression of WT-HA-KISS1R also

decreased in similar proportions ($60 \pm 2\%$, $64 \pm 5\%$, and $48 \pm 3\%$ for WT-HA + (AAA)₄, WT-HA + AAA(PRR)₃, WT-HA + Δ PRR respectively). The relative expression at the cell surface to the total expression was therefore not changed by the co-expression of a mutated receptor (Figure 7). It is important to note, (PRR)₃AAA-KISS1R had no significant effect on neither total nor cell surface expression of WT-HA-KISS1R.

DISCUSSION

Natural inactivating mutations of GPCR have long been considered as a cause of endocrine diseases (LHR, TSHR, FSHR, GnRH, GHRH, MC4R, MC2R, MC3R, CaR, PTHR1, KISS1R), retinis pigmentosa (Rhodopsin), nephrogenic diabetes insipidus (V2R) and Hirschsprung disease (ET_BR). They were also associated to susceptibility to HIV infection (CCR5), determination of skin and hair colors (MC3R) or increased susceptibility to melanoma (MC1R) (34, 35). Most of these diseases or physiological traits are transmitted as a recessive trait. In few cases, a dominant transmission has been reported (34). Loss of function mutation of KISS1R leading to isolated gonadotropic deficiency has been recently described (4, 5). Few homozygous or compound heterozygous mutations have been described in patients with recessive transmission of IHH (4, 5, 10-15). In the present study, we showed that the insertion of a PRR sequence in the intracellular domain of KISS1R disturbed the normal expression of the receptor at cell surface. The KISS1R bearing the additional PRR repeat exerts a dominant negative effect on the WT receptor expression. This additional PRR within a repetition of three consecutive PRR sequence constrained this sequence into a PPII helix and increases its rigidity. Altogether, this study highlights the possible dominant transmission of IHH due to KISS1R mutations. It also underscores the importance of a proline-arginine-rich region within the intracellular domain potentially involved in the normal folding and intracellular signaling pathways of KISS1R.

IHH due to KISS1R mutations is transmitted as a recessive trait (4, 5, 10-15). Several KISS1R-mutated cases have now been described. However, the understanding of the genotype-phenotype correlation of KISS1R mutations is not obvious, which underscores the complexity of the regulation of the gonadotropic axis by Kp. For instance, the complete inactivation of KISS1R may lead to a

severe gonadotropic deficiency with complete absence of pubertal onset (11). Similar dramatic inactivation of KISS1R may be associated to partial phenotype with incomplete pubertal progression (4, 5, 14). In one case, a pubertal delay was reported in one heterozygous parent (4). The neuroendocrine re-activation of the gonadotropic axis is progressive, starting before the appearance of the clinical signs of puberty (36, 37). This re-activation is related to the increase of Kp synthesis but also to the capacity of KISS1R to be activated by Kp (38). As the PRR insertion reduced cell surface expression of the mutant KISS1R but also the expression of WT-KISS1R by a dominant negative effect, we propose that the IHH phenotype observed in this patient is attributable to the PRR insertion. Such dominant negative effect of natural GPCR mutants on the WT receptor has already been described in TSHR, MC4R, CaR, CCR5 (34).

The repetition of 3 PRR is unique to the human KISS1R. However, this part of the intracellular domain is arginine-rich in other species (Figure 8). The arginine-rich motif RXR is considered as the core motif of endoplasmic reticulum (ER)-exit or ER-retention signals (39). Natural mutations of the RXR motif favored cell surface localization of CaR, which suggests that it may constitute an ER-retention signals for this receptor (40). Initially, we suspected that the additional PRR repeat might lead to the formation of an additional RXR motif leading to an ER-retention of the mutant receptor. Our in vitro mutagenesis of the PRR region did not support this hypothesis. Deletion of the complete PRR repetition did not lead to a higher cell surface expression of KISS1R. This arginine-rich region of the intracellular domain thus does not function as a retention signal in KISS1R.

It is now well known that during GPCR biosynthesis, dimer formation is required to pass quality control checkpoints in the ER (41). The role of GPCR dimerization in the ER quality control is complex. In some instances, the heterodimerization is required for a normal expression, whereas in other situations, heterodimerization between GPCR is deleterious. The latter has been well described for several mutated GPCRs, which generate asymmetric structures with their WT receptor and are then recognized as misfolded proteins and degraded (42). The co-expression of WT-HA-KISS1R with mutant receptors highly supports that the dimer symmetry is important for KISS1R to pass the ER quality control. Our results also show that the dominant negative effect of PRR-KISS1R on WT-KISS1R was observed for a mutant receptor bearing four alanine triplets in place of PRR repeats. The

dominant negative effect of PRR-KISS1R was thus not due to the presence of a RXR motif in the heterodimer, which had not been masked by the WT-KISS1R as described for the glutamate metabotropic receptor (43).

The lower expression at the cell surface of PRR-KISS1R homodimers without the change of the total expression suggests that PRR-KISS1R homodimers disturbed the intracellular traffic of the receptor. *In-silico* molecular dynamics indicates that the PRR insertion strongly alters the flexibility of the proline- and arginine-rich region. It underlines that WT-KISS1R proline- and arginine-rich region does not possess stable PPII conformation and is highly flexible, whereas the addition of one PRR repeat in this region forms a quite rigid sequence and a true PPII helix. We suspect that the PRR insertion could modify the interaction of the proline-arginine-rich region of KISS1R with an unknown partner protein. To date, the catalytic subunit of protein phosphatase 2A (PP2A-C) is the only protein known to physically interact with the intracellular domain of KISS1R. This interaction occurs between Arg335 and Ala358, including the PRR repetitions and seems to be involved in the anti-metastatic role of Kp (44). Additional experiments are necessary to test whether the additional PRR repeat disturbs the interaction of KISS1R with PP2A-C.

Surprisingly, our results showed that the PRR region is also involved in the signaling pathway of KISS1R. Indeed, the EC50 of (AAA)₄-KISS1R or ΔPRR-KISS1R were both increased. The sequence alignment among species of the proline- and arginine-rich region indicates that prolines are poorly conserved (Figure 8). In contrast, the Arg344 is completely conserved but also in (PRR)₃-AAA, which has the same EC50 as WT-KISS1R, suggesting that this arginine is particularly important for coupling KISS1R to Gq proteins. Additional functional analyses are needed to precisely delineate residues of this PRR region critical for the transduction pathway of KISS1R.

The present study provides the first description of a mutant KISS1R having a dominant negative effect on the WT receptor, ultimately causing IHH. It also highlights the functional importance of a proline- and arginine-rich region in the intracellular domain that appears to be involved in the folding of this domain. In respect with the abundance of arginine residues in the region of KISS1R, where the PRR insertion is located, with the important role of arginine-rich motifs in protein interactions, it would be particularly interesting to characterize proteins interacting with KISS1R in GnRH neurons.

Identification of such KISS1R protein partners could yield a better understanding of the activation of the Kp-KISS1R system at the onset of puberty.

ACKNOWLEDGMENTS

This work was supported by the Institut National de la Santé et de la Recherche Médicale and the French National Research Agency (FrenchKiss ANR-07-BLAN-0056-04).

REFERENCES

1. de Roux N, Young J, Misrahi M, Genet R, Chanson P, Schaison G, Milgrom E 1997 A family with hypogonadotropic hypogonadism and mutations in the gonadotropin-releasing hormone receptor. *N Engl J Med* 337:1597-1602
2. Bouligand J, Ghervan C, Tello JA, Brailly-Tabard S, Salenave S, Chanson P, Lombes M, Millar RP, Guiochon-Mantel A, Young J 2009 Isolated familial hypogonadotropic hypogonadism and a GNRH1 mutation. *N Engl J Med* 360:2742-2748
3. Topaloglu AK, Tello JA, Kotan LD, Ozbek MN, Yilmaz MB, Erdogan S, Gurbuz F, Temiz F, Millar RP, Yuksel B 2012 Inactivating KISS1 mutation and hypogonadotropic hypogonadism. *N Engl J Med* 366:629-635
4. de Roux N, Genin E, Carel JC, Matsuda F, Chaussain JL, Milgrom E 2003 Hypogonadotropic hypogonadism due to loss of function of the KiSS1-derived peptide receptor GPR54. *Proc Natl Acad Sci U S A* 100:10972-10976
5. Seminara SB, Messenger S, Chatzidaki EE, Thresher RR, Acierno JS, Jr., Shagoury JK, Bo-Abbas Y, Kuohung W, Schwinof KM, Hendrick AG, Zahn D, Dixon J, Kaiser UB, Slaugenhaupt SA, Gusella JF, O'Rahilly S, Carlton MB, Crowley WF, Jr., Aparicio SA, Colledge WH 2003 The GPR54 gene as a regulator of puberty. *N Engl J Med* 349:1614-1627
6. Topaloglu AK, Reimann F, Guclu M, Yalin AS, Kotan LD, Porter KM, Serin A, Mungan NO, Cook JR, Ozbek MN, Imamoglu S, Akalin NS, Yuksel B, O'Rahilly S, Semple RK 2009 TAC3 and TACR3 mutations in familial hypogonadotropic hypogonadism reveal a key role for Neurokinin B in the central control of reproduction. *Nat Genet* 41:354-358
7. Garcia-Galiano D, van Ingen Schenau D, Leon S, Krajnc-Franken MA, Manfredi-Lozano M, Romero-Ruiz A, Navarro VM, Gaytan F, van Noort PI, Pinilla L, Blumenrohr M, Tena-Sempere M 2012 Kisspeptin signaling is indispensable for neurokinin B, but not glutamate, stimulation of gonadotropin secretion in mice. *Endocrinology* 153:316-328
8. Dungan HM, Gottsch ML, Zeng H, Gragerov A, Bergmann JE, Vassilatis DK, Clifton DK, Steiner RA 2007 The role of kisspeptin-GPR54 signaling in the tonic regulation and surge release of gonadotropin-releasing hormone/luteinizing hormone. *J Neurosci* 27:12088-12095
9. Oakley AE, Clifton DK, Steiner RA 2009 Kisspeptin signaling in the brain. *Endocr Rev* 30:713-743
10. Lanfranco F, Gromoll J, von Eckardstein S, Herding EM, Nieschlag E, Simoni M 2005 Role of sequence variations of the GnRH receptor and G protein-coupled

- receptor 54 gene in male idiopathic hypogonadotropic hypogonadism. *Eur J Endocrinol* 153:845-852
11. Nimri R, Lebenthal Y, Lazar L, Chevrier L, Phillip M, Bar M, Hernandez-Mora E, de Roux N, Gat-Yablonski G 2011 A novel loss-of-function mutation in GPR54/KISS1R leads to hypogonadotropic hypogonadism in a highly consanguineous family. *J Clin Endocrinol Metab* 96:E536-545
 12. Semple RK, Achermann JC, Ellery J, Farooqi IS, Karet FE, Stanhope RG, O'Rahilly S, Aparicio SA 2005 Two novel missense mutations in g protein-coupled receptor 54 in a patient with hypogonadotropic hypogonadism. *J Clin Endocrinol Metab* 90:1849-1855
 13. Teles MG, Trarbach EB, Noel SD, Guerra-Junior G, Jorge A, Beneduzzi D, Bianco SD, Mukherjee A, Baptista MT, Costa EM, De Castro M, Mendonca BB, Kaiser UB, Latronico AC 2010 A novel homozygous splice acceptor site mutation of KISS1R in two siblings with normosmic isolated hypogonadotropic hypogonadism. *Eur J Endocrinol* 163:29-34
 14. Tenenbaum-Rakover Y, Commenges-Ducos M, Iovane A, Aumas C, Admoni O, de Roux N 2007 Neuroendocrine phenotype analysis in five patients with isolated hypogonadotropic hypogonadism due to a L102P inactivating mutation of GPR54. *J Clin Endocrinol Metab* 92:1137-1144
 15. Breuer O, Abdulhadi-Atwan M, Zeligson S, Fridman H, Renbaum P, Levy-Lahad E, Zangen DH 2012 A novel severe N-terminal splice site KISS1R gene mutation causes hypogonadotropic hypogonadism but enables a normal development of neonatal external genitalia. *Eur J Endocrinol* 167:209-216
 16. d'Anglemont de Tassigny X, Fagg LA, Dixon JP, Day K, Leitch HG, Hendrick AG, Zahn D, Franceschini I, Caraty A, Carlton MB, Aparicio SA, Colledge WH 2007 Hypogonadotropic hypogonadism in mice lacking a functional Kiss1 gene. *Proc Natl Acad Sci U S A* 104:10714-10719
 17. Lapatto R, Pallais JC, Zhang D, Chan YM, Mahan A, Cerrato F, Le WW, Hoffman GE, Seminara SB 2007 Kiss1^{-/-} mice exhibit more variable hypogonadism than Gpr54^{-/-} mice. *Endocrinology* 148:4927-4936
 18. Sykiotis GP, Plummer L, Hughes VA, Au M, Durrani S, Nayak-Young S, Dwyer AA, Quinton R, Hall JE, Gusella JF, Seminara SB, Crowley WF, Jr., Pitteloud N 2010 Oligogenic basis of isolated gonadotropin-releasing hormone deficiency. *Proc Natl Acad Sci U S A* 107:15140-15144
 19. Zhang Y 2008 I-TASSER server for protein 3D structure prediction. *BMC Bioinformatics* 9:40
 20. Fitzkee NC, Fleming PJ, Gong H, Panasik N, Jr., Street TO, Rose GD 2005 Are proteins made from a limited parts list? *Trends Biochem Sci* 30:73-80
 21. Hess B, Kutzner C, van der Spoel D, Lindahl E 2008 GROMACS 4: Algorithms for highly efficient, load-balanced, and scalable molecular simulation. *J Chem Theor Comp* 4:435-447
 22. Kabsch W, Sander C 1983 Dictionary of protein secondary structure: pattern recognition of hydrogen-bonded and geometrical features. *Biopolymers* 22:2577-2637
 23. de Brevern AG, Etchebest C, Hazout S 2000 Bayesian probabilistic approach for predicting backbone structures in terms of protein blocks. *Proteins* 41:271-287
 24. Joseph AP, Agarwal G, Mahajan S, Gelly JC, Swapna LS, Offmann B, Cadet F 2010 A short survey on protein blocks. *Biophys Rev* 2:137-145
 25. Castellano JM, Navarro VM, Fernandez-Fernandez R, Castano JP, Malagon MM, Aguilar E, Dieguez C, Magni P, Pinilla L, Tena-Sempere M 2006 Ontogeny and

- mechanisms of action for the stimulatory effect of kisspeptin on gonadotropin-releasing hormone system of the rat. *Mol Cell Endocrinol* 257-258:75-83
26. Altschul SF, Madden TL, Schaffer AA, Zhang J, Zhang Z, Miller W, Lipman DJ 1997 Gapped BLAST and PSI-BLAST: a new generation of protein database search programs. *Nucleic Acids Res* 25:3389-3402
27. Berman HM, Westbrook J, Feng Z, Gilliland G, Bhat TN, Weissig H, Shindyalov IN, Bourne PE 2000 The Protein Data Bank. *Nucleic Acids Res* 28:235-242
28. Jones DT 1999 Protein secondary structure prediction based on position-specific scoring matrices. *J Mol Biol* 292:195-202
29. Bornot A, Etchebest C, de Brevern AG 2011 Predicting protein flexibility through the prediction of local structures. *Proteins* 79:839-852
30. Roy A, Kucukural A, Zhang Y 2010 I-TASSER: a unified platform for automated protein structure and function prediction. *Nat Protoc* 5:725-738
31. Williamson MP 1994 The structure and function of proline-rich regions in proteins. *Biochem J* 297 249-260
32. Sali A, Blundell TL 1993 Comparative protein modelling by satisfaction of spatial restraints. *J Mol Biol* 234:779-815
33. Offmann B, Tyagi M, de Brevern AG 2007 Local Protein Structures. *Current Bioinformatics* 3:165-202
34. Tao YX 2006 Inactivating mutations of G protein-coupled receptors and diseases: structure-function insights and therapeutic implications. *Pharmacol Ther* 111:949-973
35. Vassart G, Costagliola S 2011 G protein-coupled receptors: mutations and endocrine diseases. *Nat Rev Endocrinol* 7:362-372
36. Manasco PK, Umbach DM, Muly SM, Godwin DC, Negro-Vilar A, Culler MD, Underwood LE 1995 Ontogeny of gonadotropin, testosterone, and inhibin secretion in normal boys through puberty based on overnight serial sampling. *J Clin Endocrinol Metab* 80:2046-2052
37. Manasco PK, Umbach DM, Muly SM, Godwin DC, Negro-Vilar A, Culler MD, Underwood LE 1997 Ontogeny of gonadotrophin and inhibin secretion in normal girls through puberty based on overnight serial sampling and a comparison with normal boys. *Hum Reprod* 12:2108-2114
38. Clarkson J, Han SK, Liu X, Lee K, Herbison AE 2010 Neurobiological mechanisms underlying kisspeptin activation of gonadotropin-releasing hormone (GnRH) neurons at puberty. *Mol Cell Endocrinol* 324:45-50
39. Michelsen K, Yuan H, Schwappach B 2005 Hide and run. Arginine-based endoplasmic-reticulum-sorting motifs in the assembly of heteromultimeric membrane proteins. *EMBO Rep* 6:717-722
40. Stepanchick A, McKenna J, McGovern O, Huang Y, Breitwieser GE 2010 Calcium sensing receptor mutations implicated in pancreatitis and idiopathic epilepsy syndrome disrupt an arginine-rich retention motif. *Cell Physiol Biochem* 26:363-374
41. Bulenger S, Marullo S, Bouvier M 2005 Emerging role of homo- and heterodimerization in G-protein-coupled receptor biosynthesis and maturation. *Trends Pharmacol Sci* 26:131-137
42. Williams D, Devi LA 2010 Escorts take the lead molecular chaperones as therapeutic targets. *Prog Mol Biol Transl Sci* 91:121-149
43. Margeta-Mitrovic M, Jan YN, Jan LY 2000 A trafficking checkpoint controls GABA(B) receptor heterodimerization. *Neuron* 27:97-106
44. Evans BJ, Wang Z, Mobley L, Khosravi D, Fujii N, Navenot JM, Peiper SC 2008 Physical association of GPR54 C-terminal with protein phosphatase 2A. *Biochem Biophys Res Commun* 377:1067-1071

ABBREVIATIONS:

NKB: neurokinin B; Kp: Kisspeptins; IHH: idiopathic hypogonadotropic hypogonadism; GPCR: G-protein coupled receptor; WT: wild type; IPs: inositol phosphate; ER: endoplasmic reticulum. PPII: polyProline II; PBs: protein blocks.

TABLES

Table 1: **Name and sequence of the proline-arginine-rich region of the different KISS1R construction.**

FIGURE LEGENDS

Figure 1: **KISS1R heterozygous mutation found in an IHH patient.** DNA was extracted from blood lymphocytes. The *KISS1R* exons were sequenced as explained in Materials and methods. A: Chromatograms showing double peaks after nucleotide 1023. Inserted nucleotides are indicated in bold and underlined. B: Protein sequence of KISS1R showing the three PRR repeats and the additional PRR in bold.

Figure 2: **The additional PRR disturbs the maximal Kp10-induced activation of KISS1R in HeLa cells.** A: IP production in WT-HA-KISS1R (black line), PRR-HA-KISS1R (gray line) and pcDNA3.1 transfected cells (dotted line) induced by 1 h incubation with Kp10. Data are shown as the mean \pm SEM of the two experiments, each performed in triplicates. B: MAPK pathway activation by a 10-min treatment with Kp10 at 10^{-5} M. The density of P-MAPK bands was quantified and normalized by the density of MAPK bands. Data are the mean of triplicates (WT-HA-KISS1R in black, PRR-HA-KISS1R in gray) (**=p<0.01, ***=p<0.001).

Figure 3: **PRR-KISS1R is poorly expressed at the cell surface.** KISS1R expression was quantified by an ELISA against the HA-tag in HeLa cells transiently expressing WT-HA-KISS1R (black bars) and PRR-HA-KISS1R (gray bars). A: Cell surface expression in the absence of triton. B: Total

expression in triton-permeabilized cells. Data are reported as the mean \pm SEM of three independent experiments, each performed in triplicates (***=p < 0.001).

Figure 4: PRR-KISS1R exerts a dominant negative effect on the expression of WT-KISS1R. A: Cell surface expression in the absence of triton. B: Total expression in triton-permeabilized cells. C: Ratio of cell surface expression on total expression. HeLa cells were co-transfected with 1.5 μ g of WT-HA-KISS1R alone or with 1 or 3 μ g of non-tagged PRR-KISS1R (black bars), or with 1.5 μ g of PRR-HA-KISS1R alone or with 1 or 3 μ g of non-tagged PRR-KISS1R (gray bars). ELISA was performed as previously described (see Material and Methods and legend to Figure 3). Data are reported as the mean \pm SEM of three independent experiments, each performed in triplicates (*: compared to WT-HA-KISS1R expression in the absence of PRR-KISS1R, §: compared to PRR-HA-KISS1R expression alone) (*=p<0.05, ***=p<0.001, §§=p<0.01).

Figure 5: The additional PRR constrains the proline-arginine rich region into a PPII helix. Two protein fragments of 24 or 27 residues were first modeled with I-Tasser. The best five structural models were selected and constrained to adopt a PPII helix conformation. Ten structural models were selected for each protein fragment. Molecular dynamic simulations were then performed with GROMACS software as described in supplementary methods. A: Distances between extremities of both protein fragments were measured (hatched line) during 50 ns. B: PBs analysis of both fragments ((PRR)₃ in the left panel and (PRR)₄ in the right panel). *a* to *p* correspond to 16 local prototypes (see supplementary methods) with PB *d* corresponds to a PPII helix. Color ranges indicated the probability to adopt a local conformation (dark blue, *i.e.*, 0 %, to red, *i.e.*, 100%). C: *Neq* for each residue in (PRR)₃ (red line) and in (PRR)₄ (blue line).

Figure 6: The dominant negative effect of the additional PRR is not due to the biochemical nature of inserted residues. A: Kp10-induced IP production in HeLa cells transiently expressing (AAA)₄, AAA(PRR)₃, (PRR)₃AAA, and Δ PRR mutated KISS1R. Data represent two experiments, performed in triplicates. B: Quantification of cell surface and total expression of mutated KISS1R and

ratio of cell surface expression on total expression. Data are reported as the mean±SEM of two experiments performed in triplicates (**=p<0.01, ***=p<0.001).

Figure 7: Ala-KISS1R-mutants exert a dominant negative effect on the WT-KISS1R cell surface expression except the (PRR)₃AAA mutant. HeLa cells were transfected with 1.5µg of HA-KISS1R, and 1.5µg of non-tagged KISS1R mutants. ELISA was performed as previously described. Data are reported as the mean±SEM of two experiments performed in triplicates (*=p<0.5, **=p<0.01).

Figure 8: The alignment of sequence of the PRR-repeat region indicates that Arg344 and Arg346 (in bold) are conserved among species and in mutant receptors.

KISS1R plasmide	Amino acid sequence of interest
WT	PRR PRR PRR
(PRR) ₄	PRR PRR PRR PRR
(AAA) ₄	AAA AAA AAA AAA
AAA(PRR) ₃	AAA PRR PRR PRR
(PRR) ₃ AAA	PRR PRR PRR AAA
ΔPRR	-

Figure 1

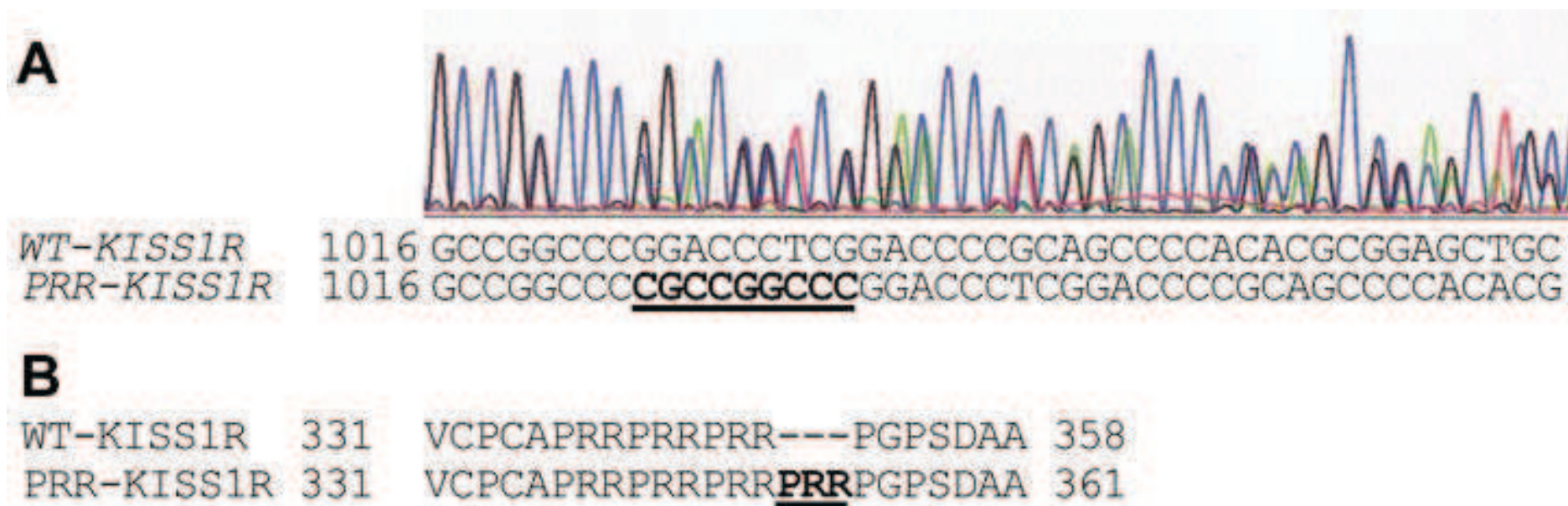
[Click here to download high resolution image](#)

Figure 2
[Click here to download high resolution image](#)

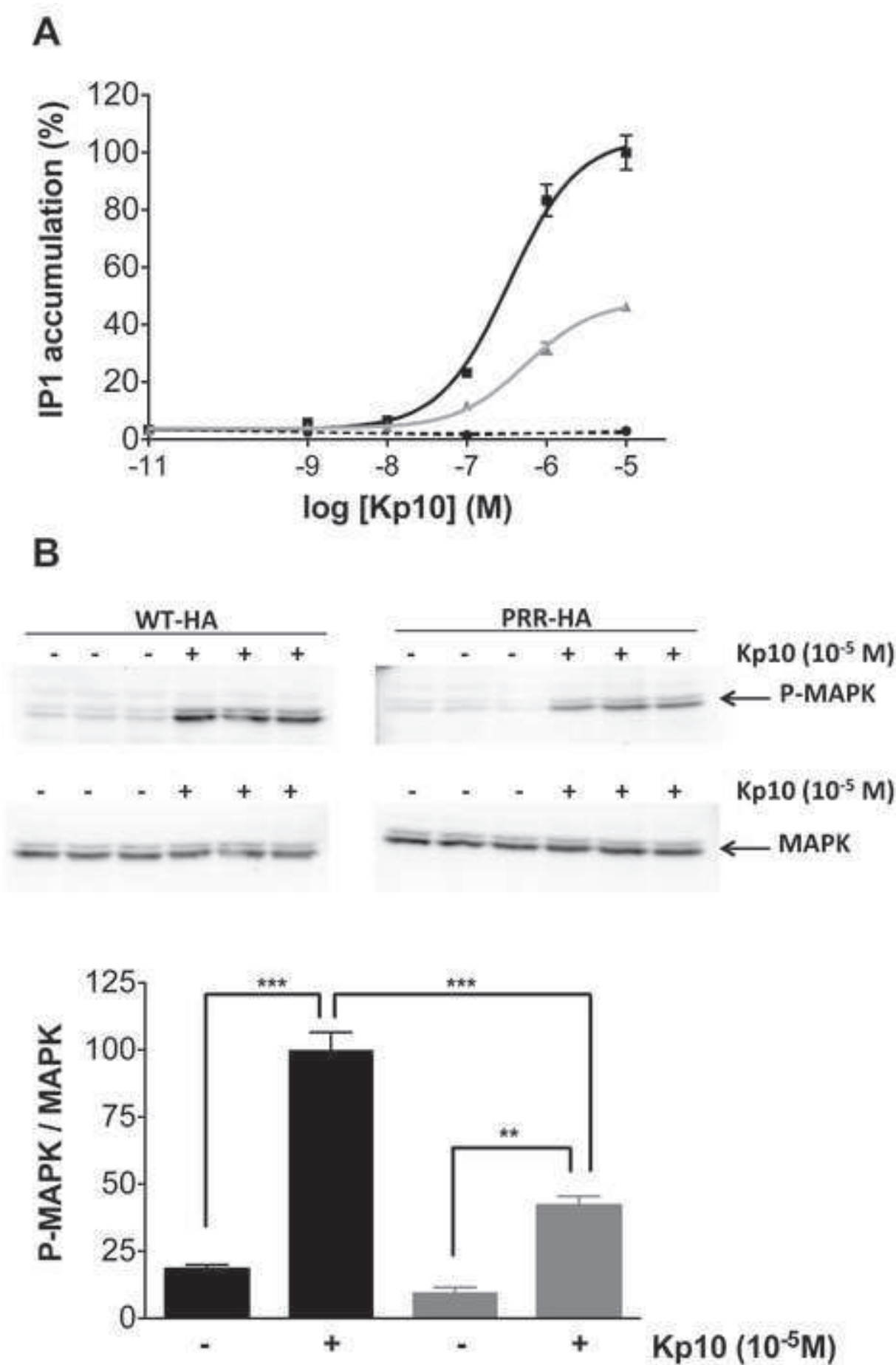


Figure 3
[Click here to download high resolution image](#)

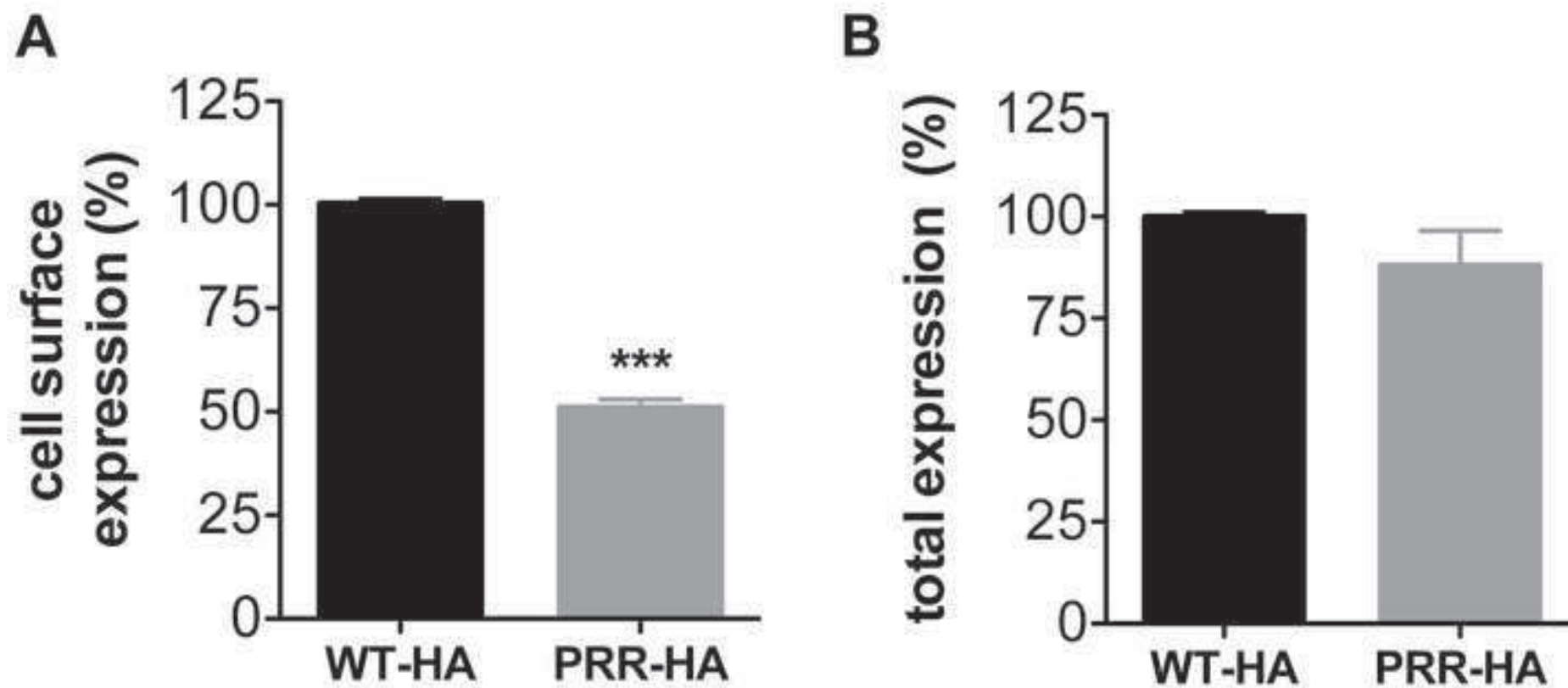


Figure 4
[Click here to download high resolution image](#)

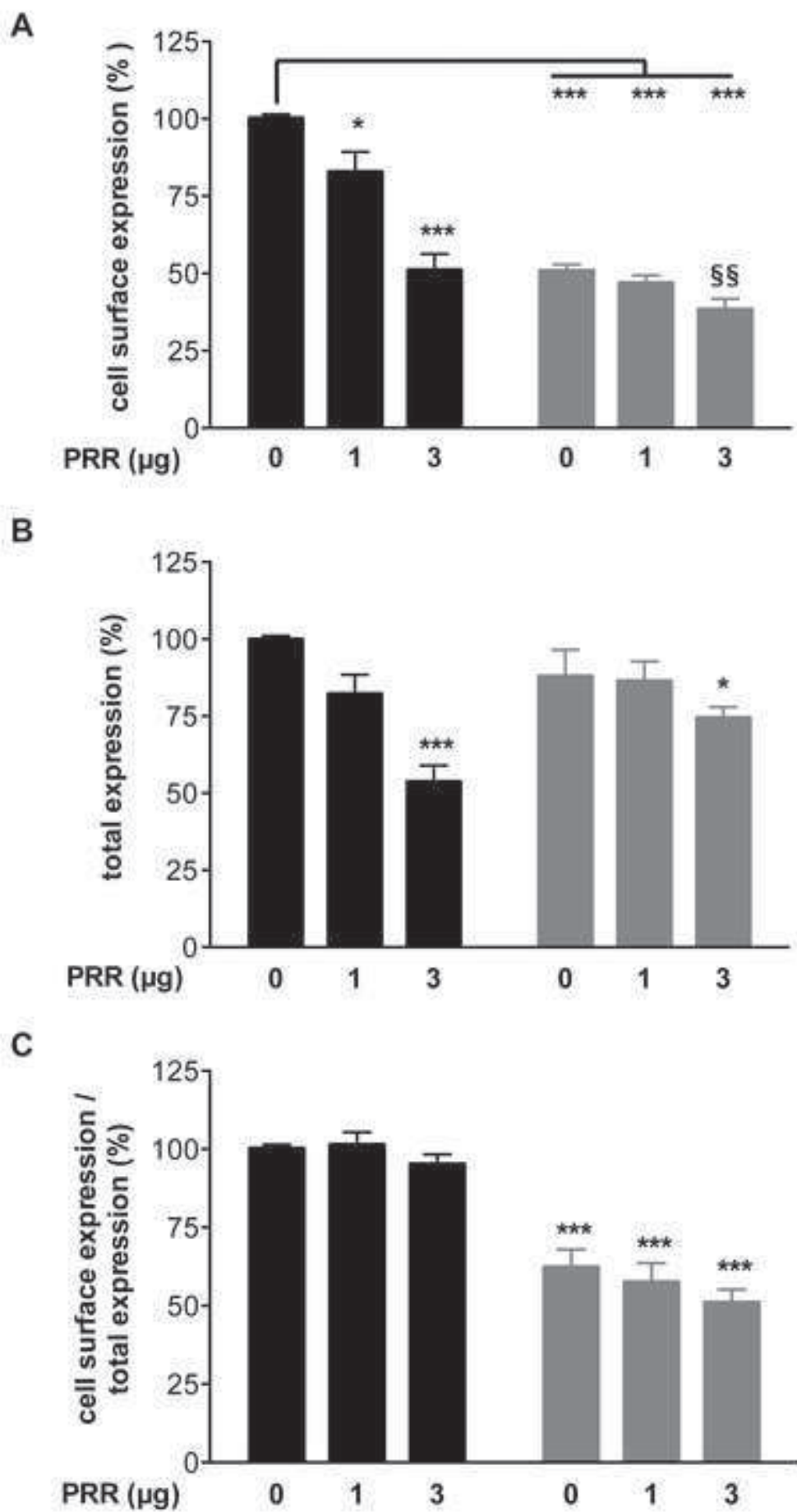


Figure 5
[Click here to download high resolution image](#)

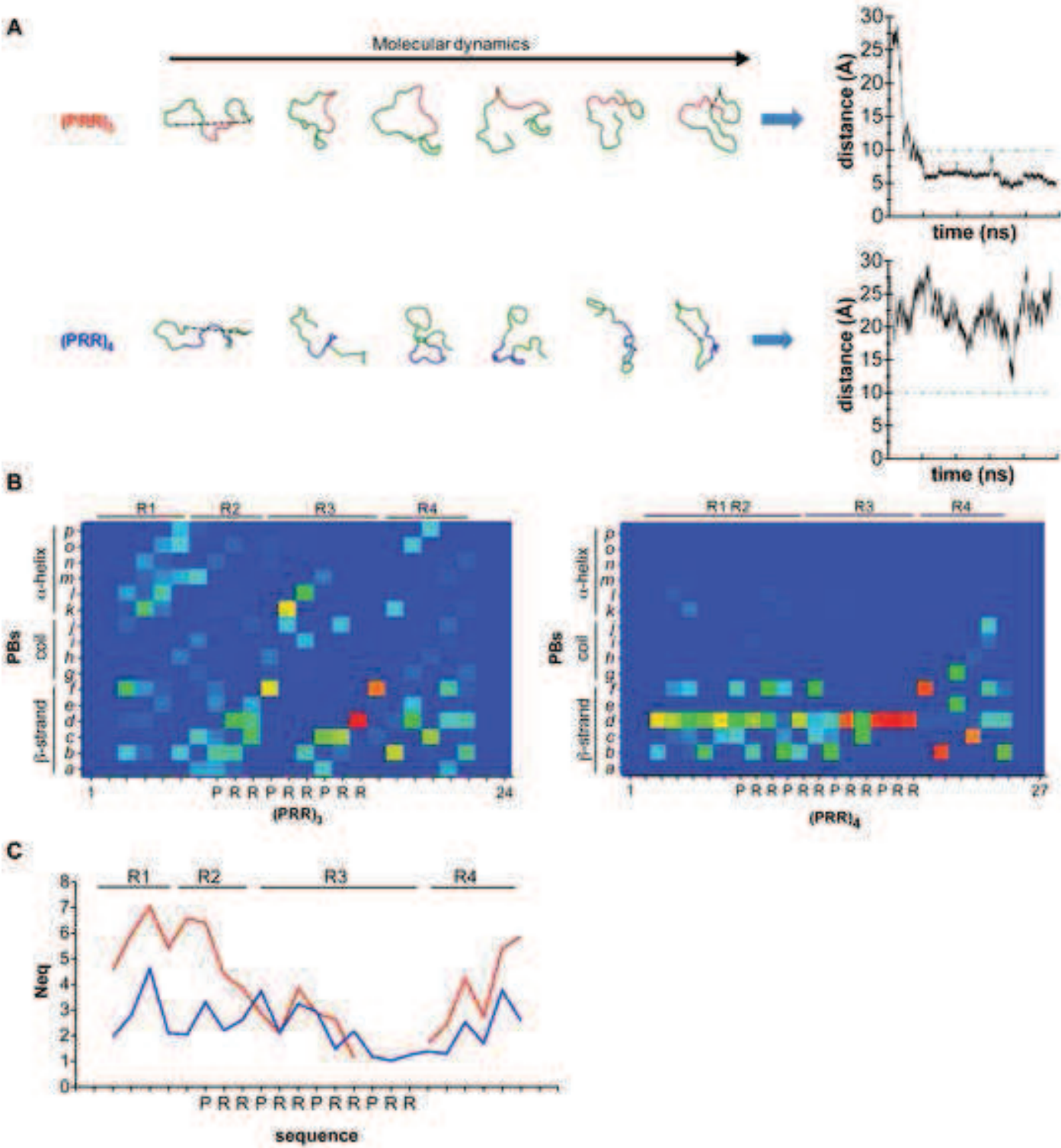


Figure 6
[Click here to download high resolution image](#)

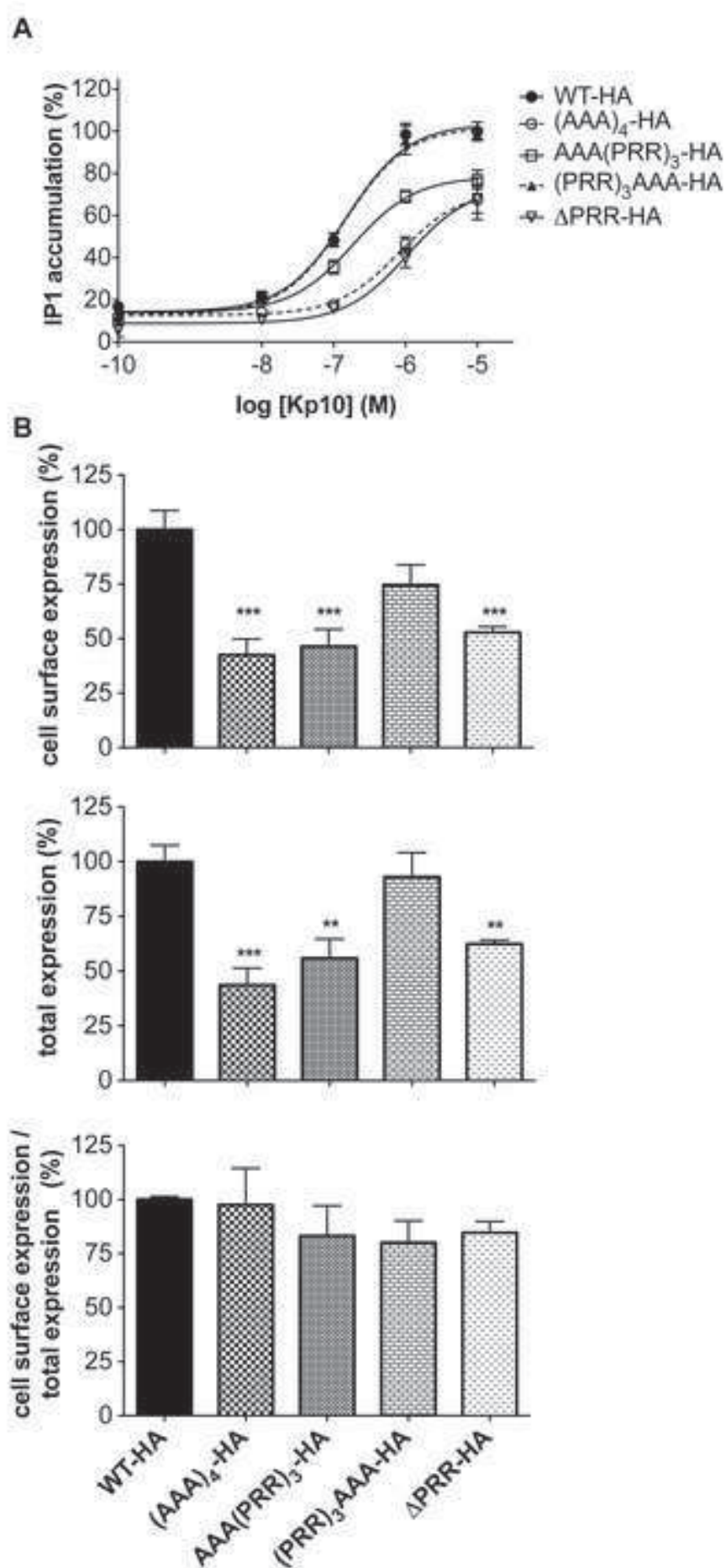


Figure 7
[Click here to download high resolution image](#)

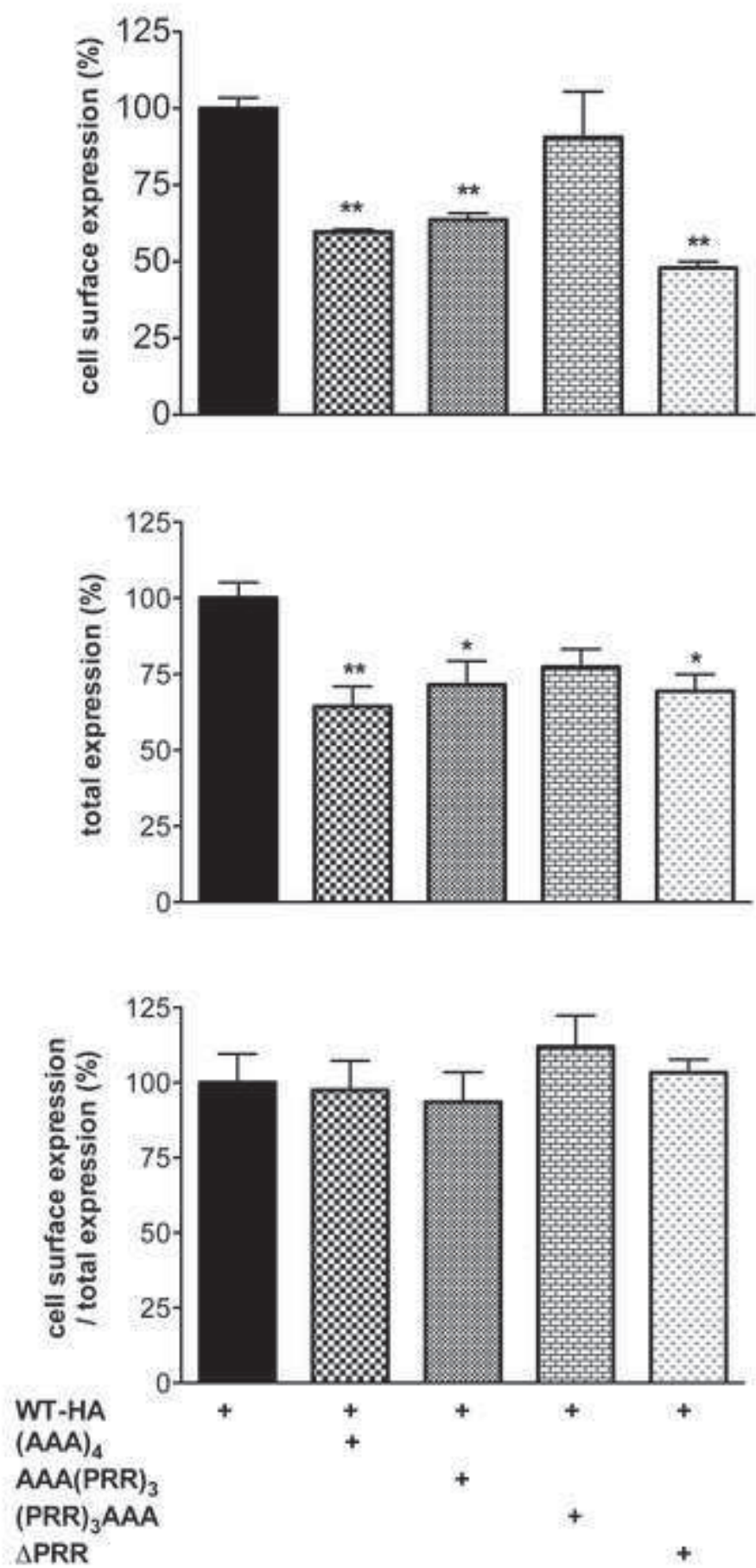


Figure 8

[Click here to download high resolution image](#)

			↓ ↓		
Homo sapiens	-(PRR) ₃	340	APRR PRR PRR---P	352	
	-(PRR) ₄	340	APRR PRR PRRPRRP	355	
	-(PRR) ₃ AAA	340	APRR PRR PRRAAAP	355	
	- AAA (PRR) ₃	340	AAAAPRRPRRPRRP	355	
Macaca falscicularis		340	APRR PR HSRR---P	352	
Rattus norvegicus		339	GPQ RQ RRPHAS---	351	
Mus musculus		340	CRQ RQ RRPHTS---	352	
Sus scrofa		340	ASRR PRRR RWS---	352	